JOURNAL OF MATERIALS SCIENCE 36 (2001) 4159–4166

Dynamic mechanical spectroscopy of plastic crystalline states in *n*-alkane systems

M. J. NOWAK, S. J. SEVERTSON
Department of Wood and Paper Science, University of Minnesota, Kaufert Laboratory, 2004 Folwell Avenue, St. Paul, MN 55108, USA

Dynamic mechanical spectroscopy (DMS) and differential scanning calorimetry (DSC) were used to study the plastic crystalline region of several model *n*-alkane systems and a commercial paraffin wax. Results indicate that DMS provides a valuable complement to existing tools for locating plastic crystalline or rotator states and characterizing the pre-melting region containing these mesophases. DMS measurements demonstrate that the mechanical properties of plastic crystalline states in *n*-alkanes are difficult to isolate, and that observed viscoelasticity surrounding the mesophases is in great part due to transitions between phases, not the rotator phases themselves. This is indicated from DMS curves that show the dynamic moduli of rotator phases are inhibited from achieving equilibrium values due to the close proximity of successive transitions. Furthermore, study of a system in which stability of a single rotator phase has been extended through strategic blending of *n*-alkanes shows that dynamic mechanical properties return to near pre-mesophase values when sufficient opportunity following a transition is provided. These results demonstrate that many *n*-alkane blends can possess a short temperature interval over which the material oscillates between Hookean and viscous behavior, controlling their performance and possibly providing for new applications requiring changes in viscoelastic properties in a narrow temperature span.

1. Introduction

A large fraction of the paraffin wax refined in the United States is sold for use as a low-cost, protective coating on boxes used to ship agricultural products. The drawback of this application is that wax-coated boxes are non-recyclable. The presence of wax coatings in recycle systems hinders production and diminishes product quality [1]. The ineffectiveness of conventional techniques at removing wax and the underlying mechanisms via which it interferes with recycling processes are not well understood, but are believed to be tied to their unique mechanical properties. What is often ignored when examining this problem is the novel phase behavior demonstrated by paraffin waxes. Bracketed between their isotropic liquid state and highly ordered crystalline phase, there often exists a series of weakly structured mesophases in which molecules in the crystals have gained a rotational degree of freedom while retaining their positional order. These states are referred to as plastic crystalline or rotator phases, and they occur at temperatures just above ambient where wax coatings are recycled. As part of a larger project on the development of environmentally benign materials, research presented here investigates the viscoelastic behavior of commercial wax coatings and model *n*-alkane compounds as a function of temperature using dynamic mechanical spectroscopy (DMS). Results presented indicate that the complex phase behavior of *n*-alkane systems can produce novel mechanical behavior in which viscoelastic properties oscillate over a small temperature region prior to the melting transition. This study also demonstrates the utility of DMS in identifying rotator phases and transitions.

1.1. Structure and thermodynamic properties of *n*-alkanes and *n*-alkane blends

Macrocrystalline or paraffin waxes are colorless, odorless materials refined from paraffinic petroleum distillates. They consist mainly of normal alkane oligomers in the C_{18} to C_{30} carbon number range, and thus their structure and properties are similar to those of *n*-alkanes and *n*-alkane blends. Phase, property and structural information on these systems comes primarily from a combination of calorimetry and x-ray diffraction. Differential scanning calorimetry (DSC) thermograms show that upon heating, macrocrystalline waxes undergo two prominent first order phase transitions (Fig. 1). The higher temperature peak is the melting transition. Most commercial paraffins melt at temperatures between 40 and 60°C depending on their carbon number distribution, with higher carbon numbers producing higher melt points. The low temperature transition has been identified as a solid-solid or polymorphic phase transition and the movement of the material into its initial rotator phase. Five unique rotator phases have been identified for *n*-alkanes, denoted R_1 through

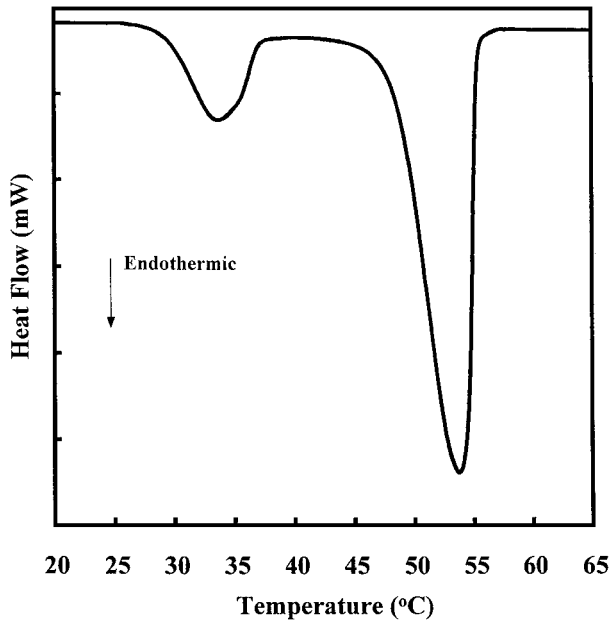

Figure 1 Differential scanning calorimetry heating curve for a typical paraffin wax showing two first order phase transitions. The first is a solid-solid transition between the orthorhombic crystal and a rotator phase. The second is the melting transition.

R_V [2]. Paraffin waxes will pass through at least one of these prior to melting. The movement between rotator phases proceeds via thermally weak first and second order phase transitions that are frequently missed with DSC. Their identification often requires the use of specialized techniques such as adiabatic calorimetry [3].

Several crystallographic studies have been published outlining structural information on the various phases that exist for *n*-alkane systems [2, 4, 5]. Prior to its solid-solid phase transition, paraffin waxes possess an orthorhombic crystal structure. Molecules in this structure are on average in a staggered conformation and arranged in a layered or lamella architecture in which their long axes lie parallel to the layer normal. In this state, the crystal possesses both positional and orientational order (rotation is inhibited by the close proximity of the carbon-hydrogen bonds of adjacent crystal members). With the onset of the solid-solid phase transition, paraffin structures, depending on carbon number distribution, will move into one of several possible rotator phase modifications. For most *n*-alkane systems this involves a distortion of the low temperature orthorhombic crystal structure. Here, the molecules retain their lamella positions but gain a rotational degree of freedom about their long axes as the free volume of the crystal increases. It is this loss of orientational order that distinguishes plastic crystals from the crystalline state. As the temperature is raised and the system moves from its polymorphic transition towards the melt, the crystal structure converts into a true hexagonal form. This transition occurs in steps that are often difficult to detect, with gradual changes in between the rotator phases. Both small- and wide-angle x-ray diffraction have been used to characterize all five *n*-alkane rotator phases [2, 4, 5]. Differences in these phases are characterized by changes in lattice constants corresponding to increases in molecular spacing and collective angle shifts. The details of which are beyond the scope of this paper.

1.2. Dynamic mechanical spectroscopy of the rotator phase region

Dynamic mechanical spectroscopy (DMS) is a familiar measurement that is common to many materials testing laboratories. It provides reliable and reproducible information on the location of transitions and has found considerable use in characterizing the viscoelastic properties of polymers as a function of temperature and frequency. Simply stated, DMS involves the introduction of an oscillatory deformation to a sample and measurement of the materials response to that deformation. Three parameters are commonly used to characterize the results, storage modulus, loss modulus and the loss tangent [6, 7]. The storage modulus (E') is a measure of the materials ability to store elastic energy and is often reported as a gauge of hardness. The loss modulus (E'') measures the freedom of molecular motion in a material, which is related to its flexibility. Finally, the loss tangent is the ratio of these quantities (i.e., ratio of loss modulus to storage modulus, or E''/E') and is often presented as the balance of viscous to elastic behavior. The loss tangent gives an indication of the cohesive strength of a material and is the quantity used to identify changes in viscoelastic behavior, such as a glass-rubber transition for a polymer [6, 8].

Given the changes that occur in its structure and properties prior to melting, a paraffin wax would be expected to provide a rich dynamic mechanical spectrum. A spectrum that is a manifestation of combined solid-rotator, rotator-rotator and rotator-liquid transformations, all occurring in a temperature span of less than 30°C. Surprisingly, it appears that little has been done in the way of characterizing the dynamic mechanical properties of *n*-alkane systems or, for that matter, any other material within their plastic crystalline region. The limited information that is available on mechanical properties of paraffins comes from blocking and needle penetration studies, which indicate that waxes simply become softer and in general demonstrate greater fluid-like behavior following their initial solid-solid transition [9–11]. These observations are in agreement with early research on plastic crystals that established their viscoelastic nature with demonstrations of greatly enhanced ability to yield and flow [12, 13]. Data presented here expands our understanding of the rotator phase region in *n*-alkanes showing it to be more complex than simply a region of increasing fluid-like behavior. Measurements were made on well-characterized model *n*-alkane systems as well as a commercially available paraffin wax coating. DMS identified known rotator phase transitions and indicates that changes in the dynamic moduli are tied primarily to phase transformations in *n*-alkane materials. Thus, paraffin waxes possess viscoelastic properties within temperature windows surrounding their phase transitions separated by regions in which the storage modulus and loss tangent have recovered partially or fully.

2. Experimental

2.1. Materials

Hydrocarbons *n*-heneicosane ($C_{21}H_{44}$) and n-tricosane ($C_{23}H_{48}$) were purchased from Roper Thermals (Clinton, CT). Purities were determined to be greater than 99% by gas chromatography. A C_{21}–C_{23} solid solution (79:21 molar ratio) was prepared by co-crystallization from the melt. X-ray diffraction confirmed that the blend was homogeneous, with no existing phase separation. The commercially available wax used in this study was Chevron Refined Wax (Chevron, San Francisco, CA), herein referred to as the commercial wax. The sample arrived in a 1-pound block, which was ground, labeled, and stored in glass jars for use in testing. Carbon number distribution results indicate that the wax is composed primarily of C_{18}–C_{30} normal alkanes (see Fig. 8).

2.2. Differential scanning calorimetry measurements

A Perkin-Elmer (Norwalk, Canada) DSC 7 thermal analyzer system controlled with Pyris Series software was used for DSC measurements. The instrument was calibrated for heat flow and temperature at 5°C/min using indium metal. An empty aluminum sample pan was used as the reference. The DSC scans for the alkanes and wax were measured by weighing approximately 8–10 mg of the sample into an aluminum hermetically sealable pan, and then placing the pan into the DSC's sample tray. The sample was heated at 5°C/min from 10°C to 60°C and then cooled back to 10°C at 5°C/min. The heating and cooling experiments were done under a nitrogen atmosphere (30 mL/min). The solid-solid and solid-liquid transition enthalpies were calculated from the area under the peaks using the Pyris software.

2.3. Dynamic mechanical spectroscopy measurements

The mechanical properties of the alkanes and wax were investigated using a Perkin-Elmer DMA 7e thermal analyzer system. Temperature calibration was performed with water, indium and zinc standards at a scan rate of 5°C/min. Pyris Series software was used to program the experiments and subsequently carry out data analysis. The method utilized for the DMS measurements involved a temperature scan from 10°C to 60°C at 5°C/min using a parallel plate fixture in compression. All experiments were normalized to the dimensions of the sample (rectangular bar, ~6 mm long × 2 mm wide × 2 mm thick). A frequency of 1.0 Hz, static stress of 2200 mN, and a dynamic stress of 2000 mN were programmed. Nitrogen was used to purge the system at a flow rate of 30 mL/min.

3. Results and discussion

This section reviews DSC and DMS results for several *n*-alkane systems. Results for model systems are presented which include pure C_{21} and C_{23} *n*-alkanes and a binary mixture of the two. These particular species compose a significant fraction of most wax coatings, and their blend produces rotator states that are stable over broad temperature regions. Locations and structures of these phases have been established in crystallographic and calorimetric studies. By matching DSC results for our samples with those found previously, the various rotator phases for the *n*-alkanes were identified and DMS was used to characterize their dynamic mechanical properties. As reviewed below, the broad rotator phases provide significant information on mesophase properties. Information that was previously masked by property changes associated with surrounding transitions. In addition to the model systems, data is also presented for a commercial paraffin wax containing a distribution of *n*-alkanes. This is a product that is commonly used in coating applications. The combination of DSC and DMS demonstrate the presence of rotator phases that have a significant impact on the mechanical properties of the material.

3.1. Thermal characterization of *n*-alkanes C_{21}, C_{23} and a C_{21}–C_{23} blend

One of the difficulties associated with characterizing rotator phases of *n*-alkanes is their close proximity to the melting transition. Typically, the temperature span between the initial solid-solid phase transition and melting, the region containing the rotator phases, is less than 30°C. This means most of the region involves the onset or completion of various first and second order transitions, making it difficult to characterize any of the phases present. For this reason, a binary mixture of pure *n*-alkanes was selected for study. Chain length mixing of normal alkanes can have a dramatic impact on the range of rotator phase stability [14], and blends of C_{21} and C_{23} *n*-alkanes provide broad temperature regions over which the material is in a single rotator phase [15]. The binary phase diagram for the mixture (Fig. 2,

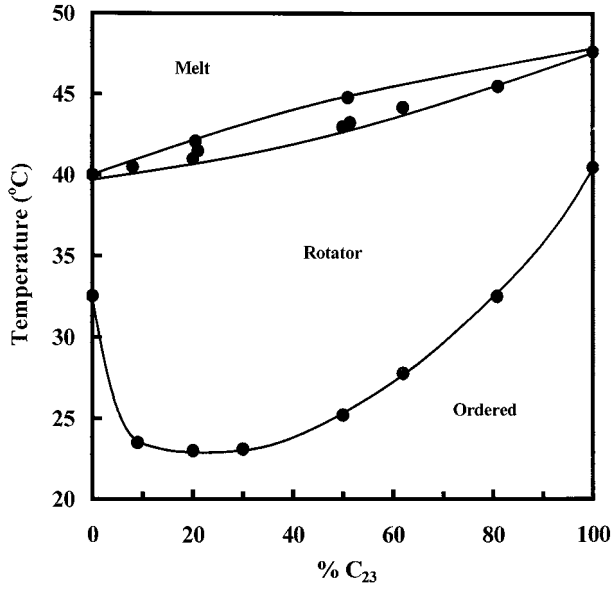

Figure 2 Binary phase diagram for the *n*-heneicosane-*n*-tricosane (C_{21}–C_{23}) system. A C_{21}–C_{23} blend in a 79:21 molar ratio maximizes the temperature range of stability for the rotator phases. Data reproduced with permission from reference 15. (Copyright 1985 American Chemical Society.)

reproduced from reference 15) shows that manipulation of the blend extends the temperature interval of rotator phases. Composition at the maximum was selected for study. It consists of a C_{21}:C_{23} blend in a 79:21 molar ratio giving a rotator phase that is stable for approximately 19°C. In addition to providing a convenient region for study, use of this particular blend has another advantage, its thermal transitions and molecular structure have been characterized in previous publications. This offers a resource to confirm the locations of transitions and allows for greater detail to be provided on the phases identified.

Shown in Fig. 3 are the DSC heating thermograms measured for C_{21} and C_{23} *n*-alkanes and the C_{21}–C_{23} blend (herein referred to as C_{21}, C_{23}, and the blend). Prior to their initial transition at low temperatures, all of the *n*-alkane systems studied here possess an orthorhombic crystal structure. As described earlier, the molecules in this structure form a lamellar architecture that is retained with modifications up through the melting transition. The first peaks on the thermograms are the polymorphic transitions, which occur at 31.6, 40.2 and 22.1°C for C_{21}, C_{23} and the blend, respectively. For both C_{21} and the blend, this is a crystal-R_1 transition. The R_1 rotator phase is the most prevalent of all rotator phase structures in *n*-alkanes. It is characterized by a rectangular or distorted-hexagonal lattice organized in a bilayer (ABA) stacking sequence [2]. This phase is the only rotator structure observed for C_{21} whereas the blend possesses an additional plastic crystalline state. For C_{23}, the solid-solid transition has been identified as a crystal-R_V transition. The R_V rotator phase is similar to the R_1 phase, i.e., it involves finite distortion of the crystal lattice and a bilayer stacking arrangement. In addition, the molecules in the R_V phase are tilted toward their nearest neighbors [2]. Unlike the first order transition between the ordered crystal and initial rotator phase characteristic of all systems presented here, movement from the R_V to R_1 phase found in C_{23} is second order and has only been resolved via high sensitivity recordings [2, 4]. The R_V phase is apparently short-lived in C_{23}. It is reported that conversion from the R_V rotator phase into the R_1 phase occurs just a couple of degrees after the solid-solid transition. Several previous studies do not identify the R_1 phase [16], with successful attempts utilizing adiabatic calorimetry [2] and DSC at a scan rate of only 1.25 K/min [4]. The existence of this transition was not evident in our DSC and DMS work, although it may be concealed by the crystal-R_V transition.

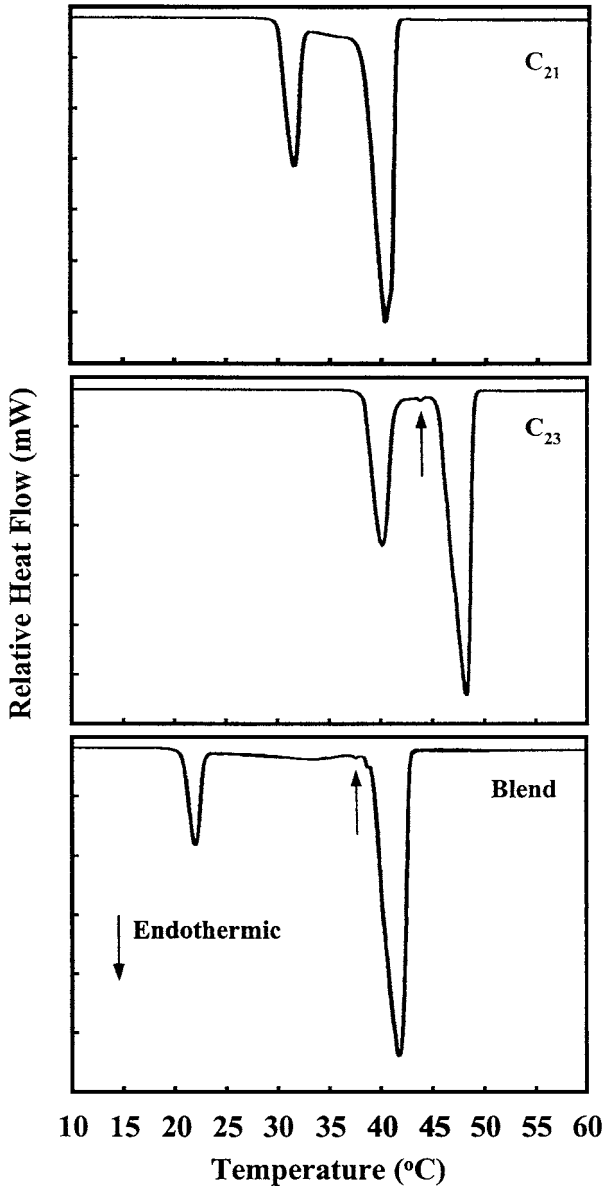

Figure 3 Differential scanning calorimetry heating curves for C_{21}, C_{23}, and a C_{21}–C_{23} blend (79:21 molar ratio). Arrows indicate the R_I–R_{II} rotator phase transformation. Blending the alkanes leads to a significant increase in the stability of the R_I rotator phase.

Prior to melting, C_{23} and the blend both undergo an additional transition. This is a R_I-R_{II} phase change that occurs at 43.8°C for C_{23} and 38.2°C for the blend. R_{II} has an average hexagonal symmetry often described as rhombohedral with a hexagonal subcell possessing trilayer (ABC) stacking [15]. Due to the small amount of heat consumed by transitions between rotator phases such as R_I-R_{II} (<1 J/g), they often go undetected by DSC. As discussed below, DMS has greater sensitivity for rotator phase transitions. Thus, as is the case for determining glass transition temperatures for many amorphous polymers, it appears a mechanical approach may be better suited for identifying the locations of these transitions. Finally, the melting transitions for C_{21}, C_{23} and the blend occur at 40.4, 48.2 and 41.7°C, respectively. The location of these transitions as well as the others identified are in agreement with those reported elsewhere [2, 17].

In addition to providing information on the locations of various transitions, thermodynamic quantities can be extracted from the DSC thermograms. The solid-solid and melting transition enthalpies calculated from the heating curves are 54 J/g and 150 J/g for C_{21}, 72 J/g and 160 J/g for C_{23}, and 29 J/g and 160 J/g for the blend. These values are consistent with those published for the pure alkanes [17] and paraffin waxes [18]. Heat capacity (C_p) is simply the derivative of the heat flow in the DSC thermograms. As was reported in several previous studies, the heat capacity shows an anomalous climb after the solid-solid transition [2, 4]. Also obtainable from

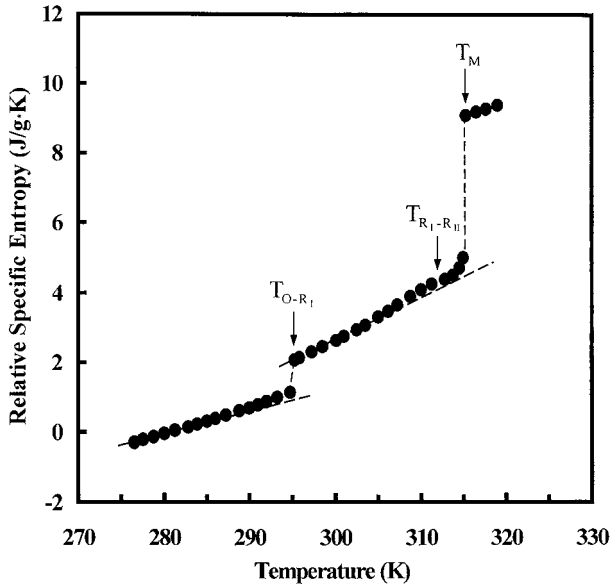

Figure 4 Relative specific entropy (arbitrary zero at 280 K) as a function of temperature for the C_{21}–C_{23} alkane blend. T_{O-R_I} = orthorhombic (O) crystal-R_I transition, $T_{R_I-R_{II}}$ = R_I–R_{II} transition, and T_M = melting transition. Data reproduced with permission from reference 15. (Copyright 1985 American Chemical Society.)

the thermograms are specific entropy values. Similar to heat capacity, specific entropy shows an unusual climb between the solid-solid and melting transitions. Fig. 4 is a plot of the relative specific entropy for the C_{21}–C_{23} blend that was reproduced from a paper that also analyzed this particular *n*-alkane system [15]. The figure demonstrates that the entropy rises rapidly with increasing temperature within the mesophase region and clearly shows the development of the transitions previously identified.

3.2. Dynamic mechanical spectroscopy of the *n*-alkanes and alkane blend

DMS curves for the *n*-alkanes are given in Figs. 5 and 6. All dynamic mechanical measurements presented cover a temperature range that begins in the materials ordered crystalline phase, passes through its rotator phase region, and ends following melting. No significant changes were observed before or after the temperature boundaries given. Fig. 5 shows the results for C_{21}. At initial temperatures, a negligible loss and high storage modulus combine to produce a small loss tangent meaning the material demonstrates little fluid-like behavior. This was found for all *n*-alkane systems tested below their solid-solid transition. The initial storage modulus for C_{21} is close to 60 MPa. This is similar to values reported for materials containing paraffin wax such as hot melt adhesives [8]. As it moves into the solid-solid (crystal-R_I) transition, starting thermally at about 25°C, there is a sharp drop in the storage modulus. This is accompanied by a moderate increase in the loss modulus and loss tangent indicating the material's becoming more viscoelastic. Increasing viscoelasticity of *n*-alkane systems as they move into their plastic crystalline states is consistent with the mechanical behavior reported in past studies [9–11]. However, the data

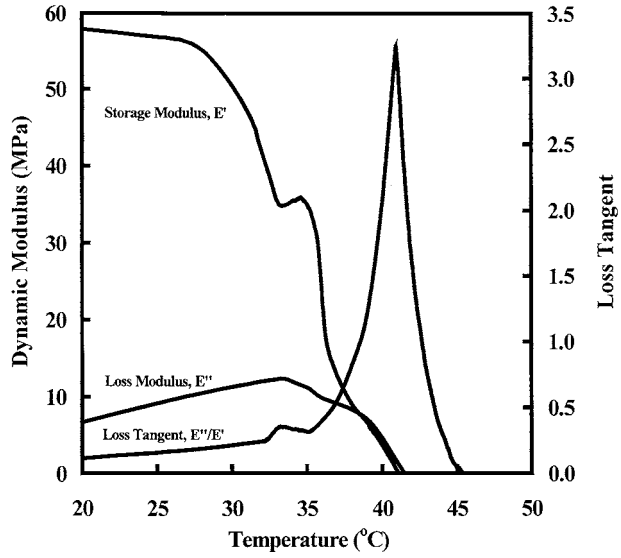

Figure 5 Dynamic mechanical heating curves for the C_{21} pure alkane.

is unusual in that an odd break appears on the storage modulus curve as it decreases, occurring at the same temperature as a local maximum in the loss tangent. Given that the break in the curve is located near the end of the crystal-R_I transition beginning thermally around 33°C, we propose that it is an indication of a recovery in the mechanical properties that is interrupted by the onset of the melting (R_I-melt) transition. In other words, the crystal-R_I and R_I-melt transitions are convoluted by their broad temperature span and close proximity, which masks the dynamic mechanical properties of the rotator phase. Examining Fig. 6, DMS data for C_{23}, the same conclusion can be drawn. The actual properties of the rotator phases are never observed due to the overlap of successive transitions. In this case, three transitions are evident from the storage modulus local minimums and loss tangent local maximums, at 42, 44 and 48°C. These correspond to the locations of the crystal-R_V (R_I), R_I-R_{II} and R_{II}-melt transitions, respectively. The only transition not observed with DMS is again the R_V-R_I transition for C_{23}.

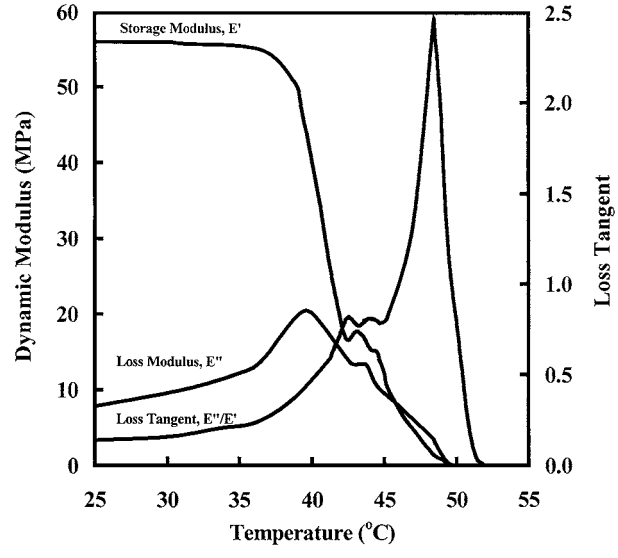

Figure 6 Dynamic mechanical heating curves for the C_{23} pure alkane.

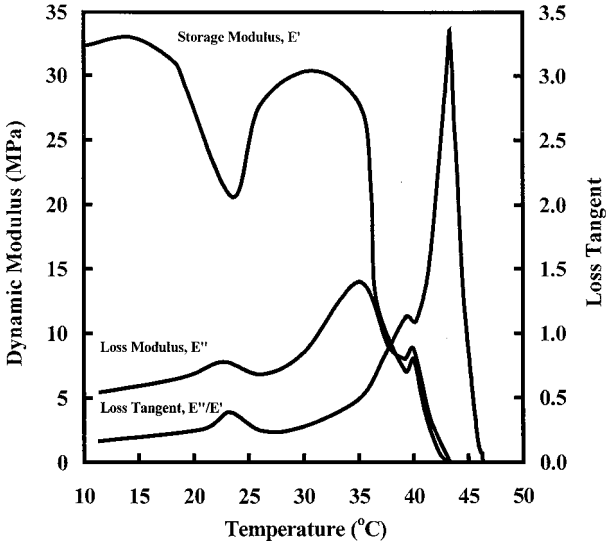

Figure 7 Dynamic mechanical heating curves for the C_{21}–C_{23} alkane blend.

The significance of the hypothesis presented above is not that materials demonstrate viscoelastic behavior during phase transitions. Loss tangent is frequently used to identify various phase transitions in polymers. Although there is little information available on the analysis of polymorphic transitions using DMS, the molecular freedom that exists during these changes should result in an identifiable peak in the loss tangent. What is significant is the implication that the rotator phases themselves may not be the fluid-like states they are believed to be. From Figs. 5 and 6, it is impossible to determine if this is correct. For these species, rotator phases are present over short temperature spans, thus the DMS curves mix and the properties of the actual rotator phases are never characterized. Attempts to isolate these properties by slowing down heating rates indicate little or no narrowing of transitions. This led to the use of the *n*-alkane blend.

As discussed, the mixing of C_{21} and C_{23} at the 79:21 molar ratio produces an R_1 rotator phase that is stable for extended temperatures. As shown in Fig. 7, the impact of broadening the rotator phase in DMS curves is significant. At initial temperatures, the storage modulus is approximately 32 MPa. This is lower than what was observed for C_{21} and C_{23}, and our data indicates that a lower initial storage modulus is typical with blended *n*-alkanes. Upon heating, the blend moves into its first transition, the crystal-R_1 phase change occurring thermally at approximately 20°C. During this transition, the storage modulus drops sharply to a local minimum of about 20 MPa at 23°C, which corresponds to a local maximum in the loss tangent. This is the same behavior seen for C_{21} and C_{23}. However, coming out of the transition, the storage modulus climbs sharply towards a local maximum of about 31 MPa close to its value prior to the transition, a climb that is accompanied by decreases in the loss tangent back to its initial value. Thus, it appears extending the R_1 rotator phase provides for a greater view of its mechanical properties, and the results indicate that this plastic crystalline state has similar viscoelastic properties as the low temperature ordered phase. The next transition, R_I-R_{II}, is close enough to the melting transition, R_{II}-melt, that the recovery of the mechanical properties is negligible, but the transitions are evident from both the storage modulus and loss tangent.

In summary, the results found with DMS for the *n*-alkanes are significant for a couple of reasons. First, they demonstrate the effectiveness of dynamic mechanical spectroscopy at determining the transitions that occur through the rotator phase region. To the best of our knowledge, DMS has not been previously used for this application, and proves to be a valuable complement to DSC for identifying these phases. Second, findings here indicate that the plastic crystalline or rotator states in *n*-alkane systems may not possess soft, fluid-like mechanical properties. Although we were only able to demonstrate the recovery of the storage modulus for the R_I rotator phase of the C_{21}–C_{23} binary mixture, the movement towards at least a partial recovery of mechanical properties following all of the phase transitions is evident. Results indicate that the reported viscoelastic behavior of some plastic crystalline phases may simply be tied to the transitions that surround them and not the actual mesophases.

3.3. Thermal and mechanical analysis of a commercial wax

In this section we characterize the thermal and dynamic mechanical properties of a commercially available paraffin wax, Chevron Refined Wax. This particular product is commonly used in the coating of corrugated boxes. Commercial paraffin waxes are composed of a broad distribution of *n*-alkanes as well as a small amount of various residual non-normal hydrocarbons. Thermal behavior of a given wax will depend primarily on its carbon number distribution. Fig. 8 is the distribution measured using GC-MS showing that the carbon

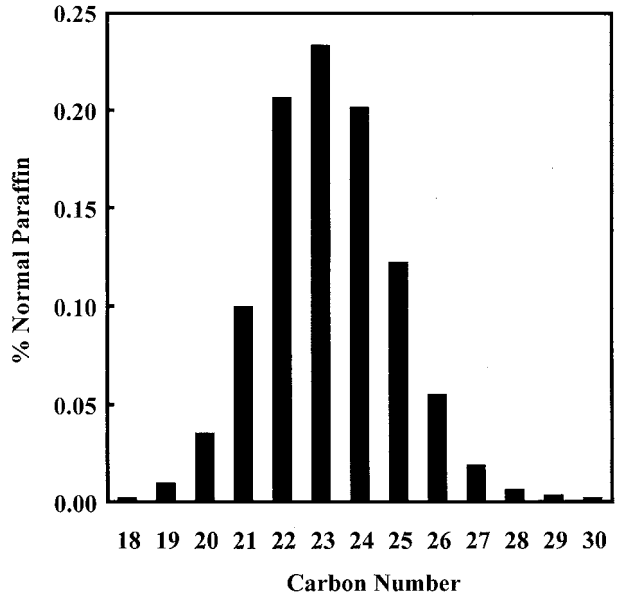

Figure 8 Carbon number distribution for the normal alkanes found in the commercial wax. (Paraffin waxes used as coatings are composed primarily of C_{18}–C_{30} *n*-alkanes. The levels of non-normal and cyclic alkanes and polymeric additives are small and not shown in this figure.)

numbers range from C_{18}–C_{30} with a majority of the *n*-alkanes falling between C_{21} and C_{26}. (Although it should be stressed that carbon number can vary from batch to batch thus affecting properties.) The DSC thermogram for this wax is shown in Fig. 9. As with the model *n*-alkane systems, the solid-solid and melting transitions are evident. There also appears to be another transition, likely an R-R transition, just after movement into the rotator phase. Analysis of x-ray diffraction patterns for this wax indicates that much like the alkane blend, the first solid-solid transition is a phase change from the low temperature orthorhombic crystal to the R_I rotator modification. The second, less endothermic transition was confirmed to be due to the R_I-R_{II} transformation. Recent studies on the phase diagrams of alkane mixtures suggest that the width of the distribution of chain lengths dramatically influences where the transitions occur [14]. In this case, the distribution spans approximately 10 carbon atoms and results in rotator phases that are very close to one another. Crystal-rotator and rotator-liquid transition enthalpies calculated from the DSC heating curve are 37 J/g and 150 J/g, respectively, and are consistent with those reported for paraffin waxes.

DMS data for the commercial wax is given in Fig. 10. As discussed, the solid-solid transition and first transition between rotator phases occur very close to each other as shown by DSC. However, only one transition is clear from the DMS data, although there does appear to be a shoulder present on the loss modulus curve centered at the correct temperature, i.e., 35–36°C. Therefore, the first major transition clearly detectable with DMS is a combination of the crystal-R_I and R_I-R_{II} phase changes ending at 39°C. This particular blend of *n*-alkanes produces a single rotator phase that is stable over an extended temperature region providing space for the storage modulus and loss tangent to make significant progress towards an equilibrium value before the next transition. (It should be noted that the scales on the loss tangent ordinate have been changed from earlier plots due to a significantly smaller loss tangent prior to melting for the commercial wax. This behavior is representative of all commercial waxes tested.) The curves demonstrate that the mechanical properties of the R_{II} phase for the commercial wax appear to be returning towards that of the pre-plastic crystalline state, an observation that was made possible by the extended rotator phase stability. The climb in the storage modulus and decrease in the loss tangent are interrupted by one final R-R transition. The transition appears to occur at 48°C and is evident from a small shoulder on the loss tangent curve and a peak in the loss modulus as they move towards their values for the melt. This transition was not detected using DSC, but x-ray diffraction confirmed that a minor structural change is occurring at this temperature. The carbon number distribution of this wax and available literature on the rotator phases of individual alkanes suggests it may be a R_{II}-R_{IV} transformation.

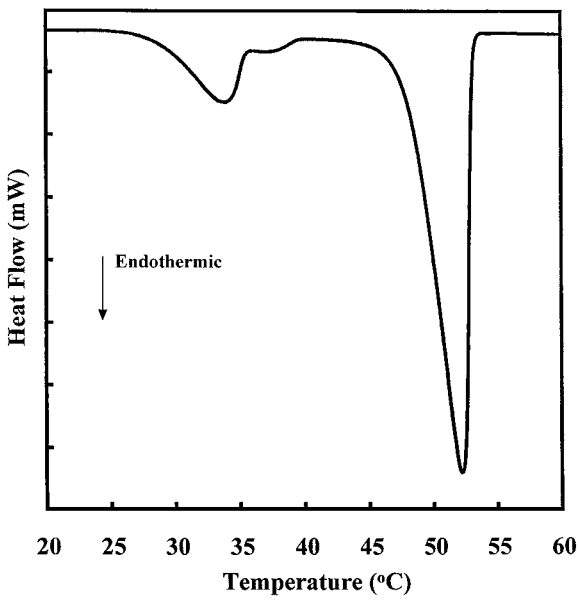

Figure 9 Differential scanning calorimetry heating curve for the commercial wax.

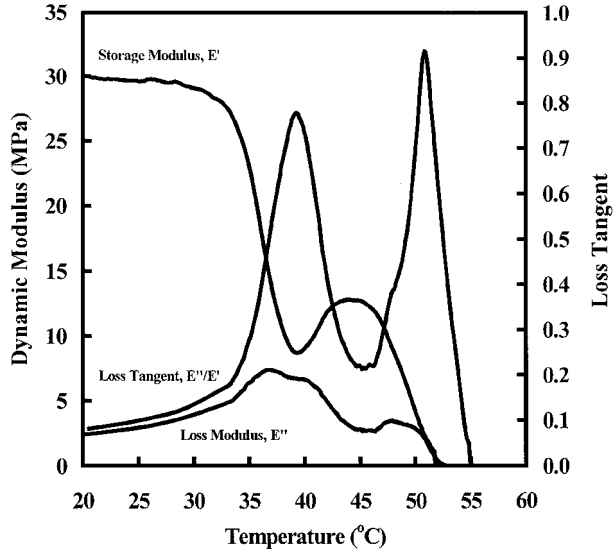

Figure 10 Dynamic mechanical heating curves for the commercial wax.

4. Conclusions

Data presented here indicates that the mechanical properties of the plastic crystalline states of *n*-alkane systems are complex. It appears that the viscoelastic behavior of rotator states may actually be governed by the transitions between phases and not the phases themselves. This conclusion is based on dynamic mechanical spectroscopy data for an *n*-alkane system showing that a broadening of the temperature range over which a single rotator phase is stable results in movement towards mechanical properties similar to its low temperature crystalline state. Thus, it is possible the fluid-like behavior reported for some plastic crystalline materials is actually a result of the convolution of successive transitions that give the appearance of a steadily increasing loss tangent following the solid-solid transition. From a practical standpoint, control over viscoelastic properties by phase transitions opens up the potential for new applications in which properties can be engineered to change over a few degrees (e.g., a switchable material). Changes in viscoelastic

properties are known to influence colloidal behavior and may be used in controlling comminution, aggregation and deposition mechanisms.

Acknowledgments

The authors thank Jamie Grunlan of the Department of Chemical Engineering and Materials Science, University of Minnesota, for use of the DMS. This research is supported by the Minnesota Agricultural Experimental Station, project number 1543-384-3650.

References

1. AF&PA/FBA SYMPOSIUM, in "Repulpable/Recyclable Treatments for Corrugated Boxes, AF&PA, Washington, DC" (FBA, Rolling Meadows, IL, 1996).
2. E. SIROTA, H. KING, D. SINGER and H. SHAO, *J. Chem. Phys.* **98** (1993) 5809.
3. E. SIROTA and D. SINGER, *ibid.* **101** (1994) 10873.
4. G. UNGAR, *J. Phys. Chem.* **87** (1983) 689.
5. J. DOUCET, I. DENICOLO and A. CRAIEVICH, *J. Chem. Phys.* **75** (1981) 1523.
6. L. H. SPERLING, "Introduction to Physical Polymer Science" (John Wiley and Sons, New York, 1992) p. 316.
7. K. P. MENARD, "Dynamic Mechanical Analysis: A Practical Introduction" (CRC Press, Boca Raton, 1999) p. 61.
8. D. BAMBOROUGH and P. DUNCKLEY, *Adhesives Age* **33** (1990) 20.
9. R. EDWARDS, *Tappi Journal* **41** (1958) 267.
10. S. SRIVASTAVA, R. TANDON, D. PANDEY, D. MADHWAL and S. GOYAL, *Fuel* **72** (1993) 1345.
11. K. ARABIAN, *Tappi Journal* **41** (1958) 275.
12. J. TIMMERMANS, *J. Phys. Chem. Solids* **18** (1961) 1.
13. L. STAVELEY, *Ann. Rev. Physical Chem.* **13** (1962) 351.
14. E. SIROTA, H. KING, H. SHAO, and D. SINGER, *J. Phys. Chem.* **99** (1995) 798.
15. G. UNGAR and N. MASIC, *ibid.* **89** (1985) 1036.
16. A. HAMMAMI and A. MEHROTRA, *Fuel* **74** (1995) 96.
17. M. FREUND, R. CSIKOS, S. KESZTHELYI and G. MOZES, "Paraffin Products: Properties, Technologies, Applications" (Elsevier Scientific, Amsterdam, 1982) p. 78.
18. R. FAUST, *Thermochimica Acta* **26** (1978) 383.

Received 8 August 2000
and accepted 26 April 2001